THE
EMBO
JOURNAL

# Dis3-like 1: a novel exoribonuclease associated with the human exosome

**Raymond HJ Staals[1],
Alfred W Bronkhorst[1], Geurt Schilders[1],
Shimyn Slomovic[2], Gadi Schuster[2],
Albert JR Heck[3], Reinout Raijmakers[3]
and Ger JM Pruijn[1],***

[1]Department of Biomolecular Chemistry, Nijmegen Center for Molecular Life Sciences, Institute for Molecules and Materials, Radboud University Nijmegen, Nijmegen, The Netherlands, [2]Faculty of Biology, Technion—Israel Institute of Technology, Haifa, Israel and [3]Biomolecular Mass Spectrometry and Proteomics Group, Bijvoet Center for Biomolecular Research and Utrecht Institute for Pharmaceutical Sciences, Utrecht University and Netherlands Proteomics Centre, Utrecht, The Netherlands

The exosome is an exoribonuclease complex involved in the degradation and maturation of a wide variety of RNAs. The nine-subunit core of the eukaryotic exosome is catalytically inactive and may have an architectural function and mediate substrate binding. In *Saccharomyces cerevisiae*, the associated Dis3 and Rrp6 provide the exoribonucleolytic activity. The human exosome-associated Rrp6 counterpart contributes to its activity, whereas the human Dis3 protein is not detectably associated with the exosome. Here, a proteomic analysis of immunoaffinity-purified human exosome complexes identified a novel exosome-associated exoribonuclease, human Dis3-like exonuclease 1 (hDis3L1), which was confirmed to associate with the exosome core by co-immunoprecipitation. In contrast to the nuclear localization of Dis3, hDis3L1 exclusively localized to the cytoplasm. The hDis3L1 isolated from transfected cells degraded RNA in an exoribonucleolytic manner, and its RNB domain seemed to mediate this activity. The siRNA-mediated knockdown of hDis3L1 in HeLa cells resulted in elevated levels of poly(A)-tailed 28S rRNA degradation intermediates, indicating the involvement of hDis3L1 in cytoplasmic RNA decay. Taken together, these data indicate that hDis3L1 is a novel exosome-associated exoribonuclease in the cytoplasm of human cells.

## Introduction

RNA is one of the most fundamental and versatile biomolecules present in the cell, with many different functions,

*Corresponding author. Department of Biomolecular Chemistry 271, Radboud University Nijmegen, PO Box 9101, Nijmegen NL-6500 HB, The Netherlands. Tel.: +31 24 361 6847; Fax: +31 24 354 0525; E-mail: G.Pruijn@ncmls.ru.nl

including the translation of genetic information into proteins, the replication of DNA and structural functions in large complexes. Perhaps one of the important features, which accounts for the diverse biological functions that can be performed by RNA, is the fact that it can be heavily modified after synthesis of the original precursors. As such, proper maturation of RNA molecules is of crucial importance for its function and can involve many different steps, such as splicing, polyadenylation, capping, as well as cleavage and/or trimming by endo- and exoribonucleases. One of the main players in the latter is the exosome, a conserved protein complex with 3′–5′ exoribonuclease activity.

Originally identified in yeast as a complex generating the 3′ end of the 5.8S rRNA in the nucleolus (Mitchell *et al*, 1997), it has become clear that the exosome complex is implicated in many processes of RNA metabolism. In the nucleoplasm and nucleolus, for instance, the maturation of many small RNAs (e.g. snRNAs and snoRNAs) is dependent on processing steps by the exosome. In addition, the exosome fulfils a function in degrading improperly processed RNAs (such as aberrant pre-mRNA and pre-tRNA species), as well as in the 'normal' turnover of cytoplasmic mRNAs (van Dijk *et al*, 2007), and it is involved in specific mRNA decay pathways, including non-stop decay and nonsense-mediated decay (van Hoof *et al*, 2002; Schilders *et al*, 2006).

The doughnut-shaped core of the exosome consists of nine proteins, six of which are homologous to the 3′–5′ exonuclease RNase PH and three proteins with RNA-binding domains (each containing an S1 RNA-binding domain and two of which contain an additional KH domain). Although the archaeal and probably also the plant exosome core seem to have retained their activity during the course of evolution, reconstitution experiments showed that the core of the yeast and human exosome are catalytically inactive (Chekanova *et al*, 2000; Lorentzen *et al*, 2005; Liu *et al*, 2006). However, two other types of hydrolytic RNases associated with exosome complexes in eukaryotes are thought to be responsible for the activity of the complex. Rrp6 (designated PM/Scl-100 in humans), an enzyme belonging to the RNase D family of hydrolytic exoribonucleases, associates with a subset of exosome cores and contributes to its activity (Brouwer *et al*, 2001b; Synowsky *et al*, 2009). Rrp6 has been reported to reside exclusively in the nucleus of yeast cells (Allmang *et al*, 1999b), whereas in human cells, PM/Scl-100 was found both in the nucleus and cytoplasm (Brouwer *et al*, 2001a; Lejeune *et al*, 2003). Depletion of Rrp6 from cells has been shown to give rise to phenotypes markedly different from when core exosome components are depleted in various experimental setups, suggesting that its function is at least partially uncoupled to that of the core exosome (van Dijk *et al*, 2007; Callahan and Butler, 2008; Graham *et al*, 2009).

Another hydrolytic exoribonuclease, Dis3 (also known as Rrp44), which belongs to the RNase R family of RNases, was recently shown to be essential for the activity of the yeast exosome (Dziembowski *et al*, 2007). In yeast, the Dis3

protein can be detected in both the nucleolus as well as the cytoplasm (Synowsky *et al*, 2009). Recently, Dis3 was found to display endonuclease activity as well, in agreement with the presence of a functional PilT N-terminus (PIN) domain in its N-terminal region (Lebreton *et al*, 2008; Schaeffer *et al*, 2009). The recently determined crystal structure of the yeast Dis3–Rrp41–Rrp45 complex led, in combination with the results of biochemical analyses, to a model in which RNA substrates thread through the central channel of the exosome core to reach the Dis3 exoribonuclease site (Bonneau *et al*, 2009).

Although a human homologue of Dis3 was described more than a decade ago and was shown to complement yeast Dis3 (Shiomi *et al*, 1998), a stable association of this protein with the exosome core could not be shown (Chen *et al*, 2001) (Schilders *et al*, in preparation; see also Supplementary Data). During our studies to identify proteins stably associated with the human exosome core, we detected another homologue of the yeast Dis3 protein, designated Dis3-like exoribonuclease 1 (Dis3L1). Here, we characterize its association with the exosome core, its subcellular localization and its enzymatic activities.

## Results

### Identification of Dis3L1 as a novel exosome-associated protein

To identify proteins associated with the core of the human exosome, which may be involved in its exoribonuclease activity or the regulation thereof, antibodies to a core component were used to isolate exosome complexes by immuno-affinity chromatography. These complexes were isolated from total HeLa cell extracts using polyclonal anti-hRrp40 antibodies (Brouwer *et al*, 2001a). Proteins that remained bound to the immobilized antibodies at 1 M NaCl were eluted and analysed by SDS–PAGE. After Coomassie Brilliant Blue staining, the gel lane was cut in 19 slices, which were subjected to in-gel digestion and analysed by nano-reversed phase liquid chromatography coupled to a high-resolution LTQ-Orbitrap mass spectrometer. Analysis of the resulting MS/MS spectra against the Swissprot database using Mascot revealed the presence of all nine core exosome subunits (Table I), as well as two additional proteins, known to associate with the exosome: PM/Scl-100 and MPP6. MPP6 has earlier been shown to be involved in the exosome-mediated maturation of the 5.8S rRNA (Schilders *et al*, 2005). The sequence coverage of the identified exosome

proteins ranged from 7 to 44%. In accordance with the earlier results, no peptides indicating the presence of the human Dis3 protein (hDis3) in the exosome preparation were detected. However, we identified with very high confidence (26% coverage and 29 unique peptides) a protein homologous to Dis3 that was designated human Dis3-like exonuclease 1 (hDis3L1).

In the genome of human beings and other higher eukaryotes (including mice, zebrafish and frogs), in total three genes homologous to the yeast Dis3 protein are present: Dis3, Dis3-like exonuclease 1 (Dis3L) and Dis3-like exonuclease 2 (Dis3L2), of which only Dis3L1 was found in the immuno-affinity-purified exosome fraction. On the basis of cDNA sequence data 4 isoforms of hDis3L1 can be discerned, which are most likely resulting from alternative splicing events. The largest isoform (GenBank acc. nr. NM_001143688) consists of 1054 amino acids with a calculated molecular mass of 120 787 Da. For the human Dis3L2 (hDis3L2), five potential isoforms have been identified, the largest of which (GenBank acc. nr. NM_152383) contains 885 amino acids with a calculated molecular mass of 99 210 Da. An alignment (Edgar, 2004; Waterhouse *et al*, 2009) of the 'canonical' isoforms of the three human Dis3 variants and their yeast equivalent (yDis3) is shown in Supplementary Figure S1. In terms of sequence conservation, hDis3 is more closely related to yDis3 (42% sequence similarity) than the two Dis3-like proteins (29 and 26% for hDis3L1 and hDis3L2, respectively). To obtain insight into the domain structure of these proteins, their amino-acid sequences were analysed by the online tool SMART (Letunic *et al*, 2009). This revealed the presence of several domains, some of which were, however, poorly conserved. Similar to many members of the RNase II/R family of hydrolytic nucleases, the three hDis3 variants contain a highly conserved RNB domain (which is known to contain the exonuclease activity) and three OB-fold-type nucleic acid-binding domains: two cold shock domains and one S1 RNA-binding domain. The conservation of the latter domains is generally more evident at the secondary structure level than at the level of the amino-acid sequence (Theobald *et al*, 2003). All β-strands and α-helixes detected in hDis3L1 with the PsiPred protein structure-prediction tool are depicted below the alignment (Supplementary Figure S1). Typical for OB-fold-like domains are the five β-strands forming a β-barrel. Finally, a PIN domain is present in the N-terminal regions of hDis3 and yDis3. PIN domains were originally thought to be involved in signalling events (Noguchi *et al*, 1996), but were recently shown to confer

**Table I** Exosome-associated proteins identified by LC-MS/MS in immunoaffinity-purified human exosome complexes

| Gene | Accession no. | Protein name(s) | MW (kDa) | Unique peptides | Sequence coverage (%) |
|------|---------------|-----------------|----------|-----------------|------------------------|
| EXOSC1 | Q9Y3B2 | hCsl4 | 21 | 4 | 25 |
| EXOSC2 | Q13868 | hRrp4 | 33 | 3 | 11 |
| EXOSC3 | Q9NQT5 | hRrp40 | 30 | 15 | 38 |
| EXOSC4 | Q9NPD3 | hRrp41 | 26 | 6 | 29 |
| EXOSC5 | Q9NQT4 | hRrp46 | 25 | 4 | 14 |
| EXOSC6 | Q5RKV6 | hMtr3 | 28 | 8 | 24 |
| EXOSC7 | Q15024 | hRrp42 | 32 | 11 | 36 |
| EXOSC8 | Q96B26 | hRrp43/OIP2 | 30 | 11 | 33 |
| EXOSC9 | Q06265 | hRrp45/PM/Scl-75 | 49 | 5 | 12 |
| EXOSC10 | Q01780 | hRrp6/PM/Scl-100 | 101 | 5 | 7 |
| MPHOSPH6 | Q99547 | MPP6 | 19 | 6 | 44 |
| DIS3L | Q8TF46 | hDis3L1 | 121 | 29 | 26 |
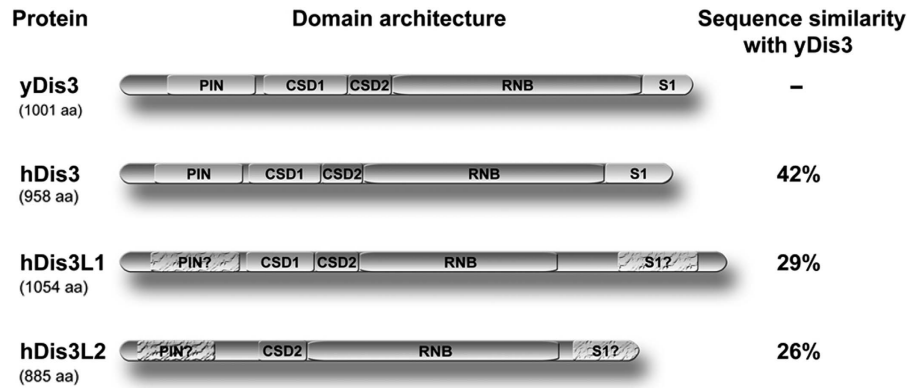
**Figure 1** Schematic structure of Dis3 and Dis3-like proteins in yeast and human beings. Schematic diagram of *S. cerevisiae* Dis3 (yDis3), human Dis3 (hDis3), human Dis3-like 1 (hDis3L1) and human Dis3-like 2 (hDis3L2) with the identified domains indicated: the PIN domain, two cold shock domains (CSD1, CSD2), an RNB domain and an S1 RNA-binding domain. Crackled boxes and question marks indicate domains with a low level of conservation (see Supplementary Figure S1 for details). The level of sequence similarity between the human Dis3 proteins and yDis3 is indicated on the right.

endonucleolytic activity. This was shown for several proteins involved in NMD and RNAi pathways, such as the SMG protein (Clissold and Ponting, 2000; Glavan *et al*, 2006) and yDis3 (Lebreton *et al*, 2008). PIN domains are characterized by two or three nearly invariant aspartic acid residues. Both hDis3 and yDis3 contain all three aspartic acids, whereas in hDis3L1 only two and in hDis3L2 only one of these residues are conserved (Supplementary Figure S1). The domain structure of yDis3, hDis3, hDis3L1 and hDis3L2 is schematically illustrated in Figure 1.

To confirm the interaction of hDis3L1 with the exosome, the full-length coding sequence of the largest isoform of hDis3L1 was cloned from a teratocarcinoma cDNA library and was inserted in different mammalian expression vectors. HEp-2 cells were transiently transfected with a construct expressing hDis3L1 fused to either a N- or C-terminal GFP tag. After 48 h, the fusion proteins were immunoprecipitated from cell lysates using anti-GFP antibodies and analysed by SDS–PAGE and immunoblotting. The results showed that both the N- and C-terminally GFP-tagged hDis3L1 proteins were expressed, although the expression of the C-terminally tagged protein was less efficient. The association with the exosome core was monitored by anti-hRrp4 antibodies and showed the co-precipitation of hRrp4 with both hDis3L1 fusion proteins, but not with GFP alone (Figure 2), confirming the interaction between hDis3L1 and the core of the exosome complex. To rule out the possibility that this interaction is mediated by RNA, similar experiments were performed in which either the cell lysates or the immunoprecipitates were treated with nucleases (RNase A and micrococcal nuclease). The co-precipitation of hRrp4 was not affected by these treatments (data not shown), indicating that the association of hDis3L1 with the exosome core is not bridged by RNA.

### hDis3L1 is localized to the cytoplasm

To analyse the subcellular localization of hDis3L1, human HEp-2 cells were transiently transfected with constructs encoding either GFP-hDis3L1, hDis3L1-GFP or VSV-hDis3L1, the latter resulting in the formation of an N-terminally VSV-tagged (vesicular stomatitis virus G epitope) protein. The localization of tagged hDis3L1 was determined by fluorescence microscopy either directly (EGFP tagged;
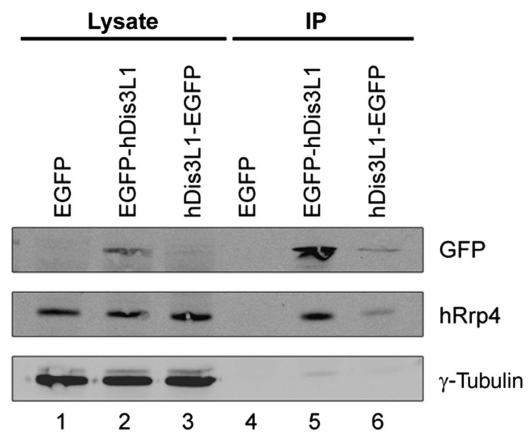


**Figure 2** Association of hDis3L1 with the exosome core complex. Total cell extracts were prepared from HEp-2 cells transiently transfected with expression constructs encoding EGFP, EGFP-hDis3L1 or hDis3L1-EGFP, after which immunoprecipitation was performed using polyclonal anti-GFP antibodies. Both the complete cell extracts (Lysate) and the anti-GFP (co-)precipitated proteins (IP) were separated by SDS–PAGE and analysed by western blotting, using monoclonal anti-GFP antibodies and monoclonal anti-hRrp4 antibodies to visualize the co-precipitation of the exosome core complex with hDis3L1. Monoclonal anti-$\gamma$-tubulin antibodies were used as loading control.

Figures 3A and B) or indirectly (VSV tagged; Figure 3C) using anti-VSV-tag antibodies. All three tagged hDis3L1 proteins localized exclusively to the cytoplasm (Figures 3A–C). To compare its localization with that of hDis3, we also transfected cells with N-terminally GFP-tagged hDis3, the localization of which was confined to the nucleoplasm (Figure 3D), in agreement with our earlier observations (Schilders *et al*, in preparation). As the localization of over-expressed, tagged proteins may not completely reflect the localization of the corresponding endogenous proteins, the subcellular localization of hDis3L1 was also determined by confocal immunofluorescence microscopy using antibodies to hDis3L1 (Figures 3E–G). Antibodies to exosome core component hRrp40 were used in parallel (Figures 3H–J). Although some staining of hDis3L1 within the nucleus was observed, the results of these experiments confirm the
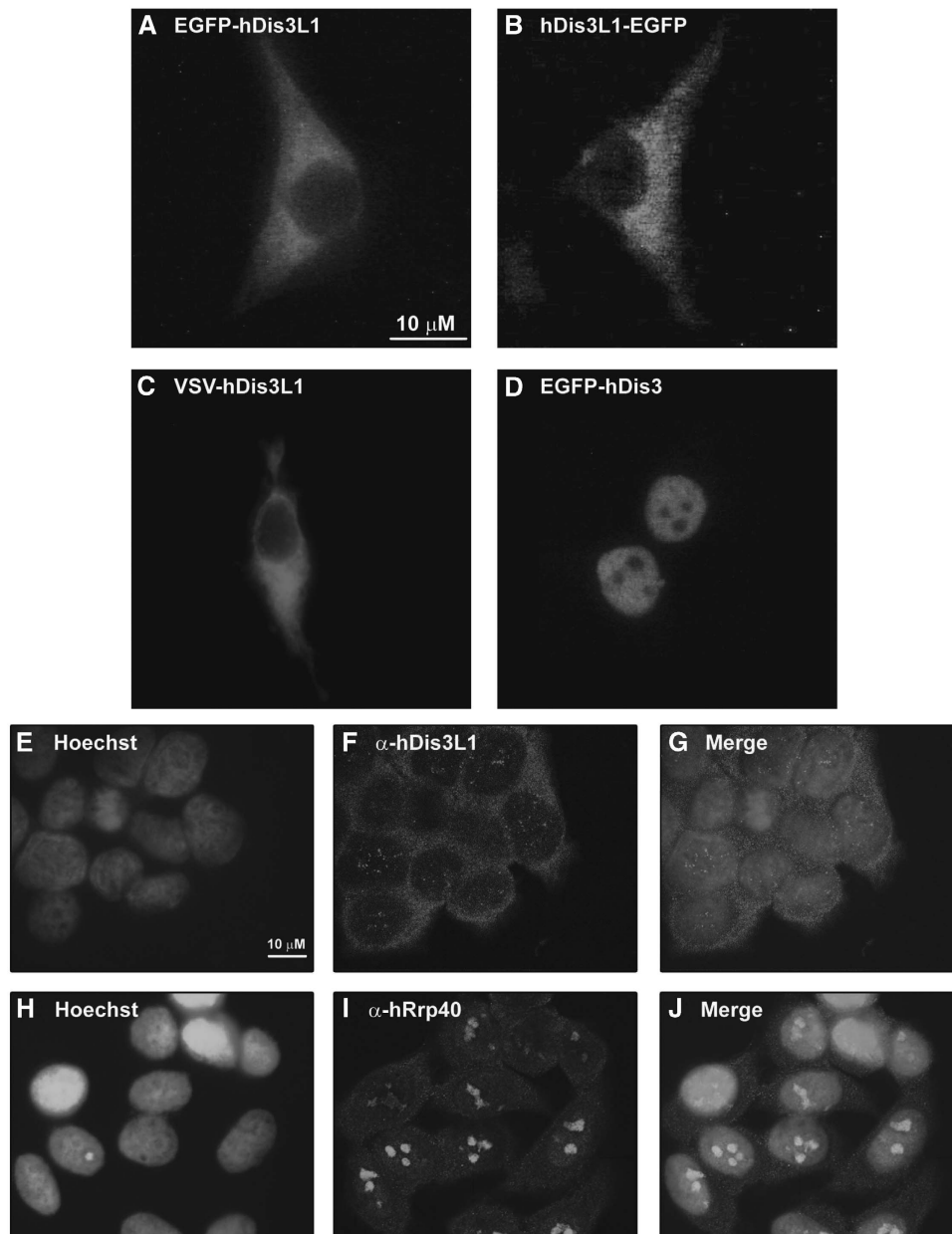
**Figure 3** Localization of hDis3L1 and hDis3 in HEp-2 cells. HEp-2 cells were transiently transfected with expression constructs encoding EGFP-hDis3L1 (**A**), hDis3L1-EGFP (**B**), VSV-hDis3L1 (**C**) or EGFP-hDis3 (**D**). Forty-eight hours after transfection, the cells were fixed and EGFP-fusion proteins were visualized directly by fluorescence microscopy. The VSV-tagged hDis3L1 protein was visualized by incubating the cells with monoclonal anti-VSV-tag antibodies, followed by Alexa Fluor 555-conjugated goat anti-mouse antibodies and fluorescence microscopy. (**E–J**) Fixed HEp-2 cells were incubated with polyclonal antibodies to hDis3L1 (**F–G**) or to hDis3 (**I–J**) and bound antibodies were visualized by Alexa Fluor 488-conjugated secondary antibodies and confocal immunofluorescence microscopy. Nuclei were visualized by Hoechst staining (**E**, **H**). (**G**) and (**J**) show the merged images of Hoechst and antibody staining. Bar: 10 μm.

cytoplasmic accumulation of hDis3L1. In agreement with earlier observations, the highest concentration of hRrp40 was observed in the nucleoli.

### hDis3L1 displays exoribonuclease activity

The lack of exoribonuclease activity associated with the core of the human exosome raised the question whether the exosome-associated hDis3L1 protein might be responsible for at least part of the activity of the human exosome. This would be consistent with the presence of the RNase II-type RNB domain in this protein. To test this hypothesis, RNA degradation assays were performed with GFP-hDis3L1

immunoaffinity purified from transiently transfected HEp-2 cells. After immunoprecipitation with anti-GFP antibodies, the precipitate was incubated for 2 h with a radiolabelled RNA substrate in the presence of various concentrations of $Mg^{2+}$, which is known to be involved in the nucleophilic attack by these types of hydrolytic enzymes (Frazao *et al*, 2006). Denaturing gel analysis of the reaction products (Figure 4A) showed that the substrate RNA indeed was converted to mononucleotides, more specifically nucleotide monophosphates, by EGFP-hDis3L1-containing precipitates, whereas no activity was found in EGFP precipitates. The activity appeared to be dependent on the $Mg^{2+}$ concentration
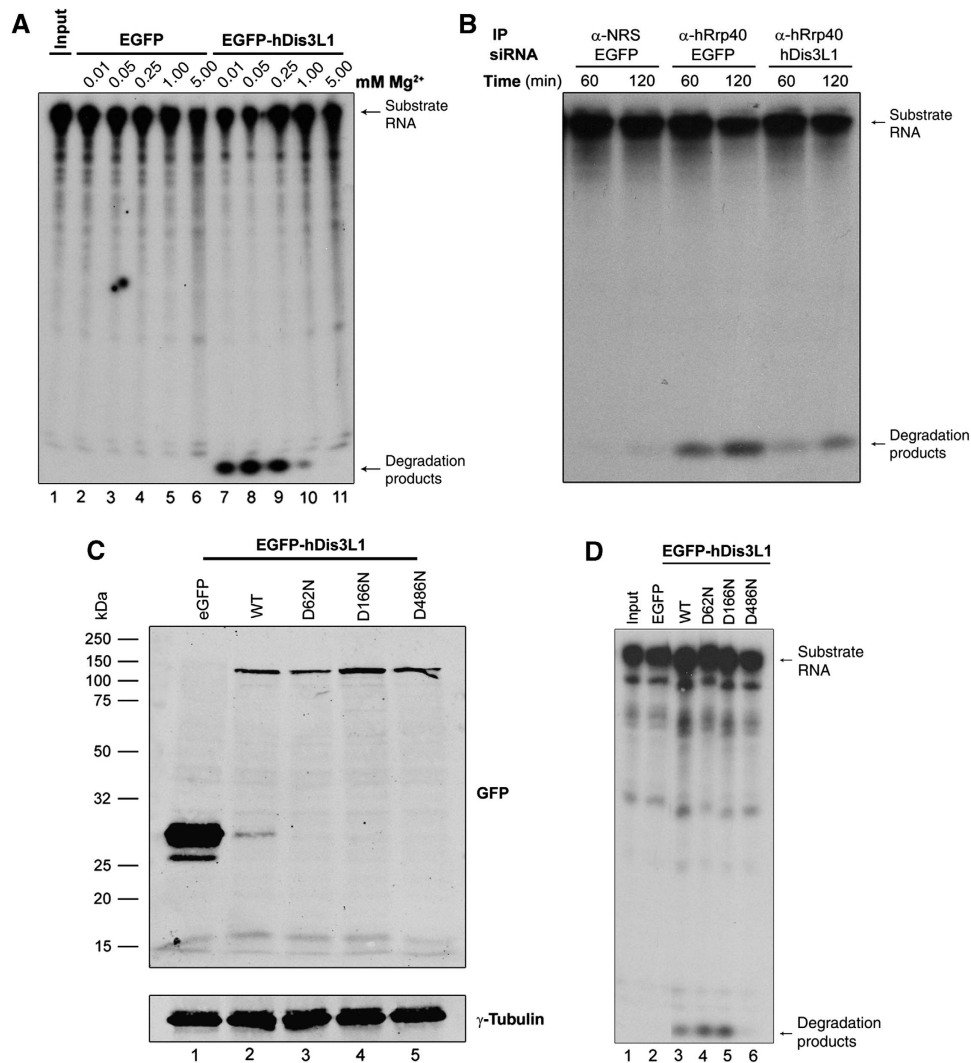
**Figure 4** *In vitro* RNA degradation by hDis3L1. (**A**) HEp-2 cells were transfected with expression constructs encoding EGFP-hDis3L1 or EGFP, and after 48 h, cell lysates were subjected to immunoprecipitation with anti-GFP antibodies. Precipitated proteins/complexes were incubated with a radiolabelled RNA substrate (Input) and the reaction products were subsequently analysed by denaturing polyacrylamide gel electrophoresis followed by autoradiography. The incubations were performed in the presence of increasing concentrations of $Mg^{2+}$. (**B**) A similar assay was performed with endogenous exosome complexes after precipitation with anti-hRrp40 antibodies or antibodies from normal rabbit serum (NRS) and lysates from cells, which were transfected with siRNAs downregulating either EGFP (used as a control) or hDis3L1. (**C**) Expression efficiency of EGFP-tagged hDis3L1 proteins monitored by western blotting using anti-GFP antibodies. WT: wild-type hDis3L1. D62N, D166N, D486N: hDis3L1 amino-acid substitution mutants. Anti-γ-tubulin antibodies were used as a loading control. (**D**) Activity assay as described above (**A**) with immunoprecipitated hDis3L1 mutants D62N, D166N, D486N in the presence of 0.05 mM $Mg^{2+}$. Precipitates from cell lysates containing EGFP and wild-type (WT) hDis3L1 were used as negative and positive control, respectively.

with an optimum at about 0.05 mM, which is very similar to the optimal $Mg^{2+}$ concentration described for yeast Dis3 (Dziembowski *et al*, 2007). To further show that the mono-nucleotide products were resulting from the presumed 3′–5′ exoribonuclease activity of EGFP-hDis3L1, the radiolabelled substrate was pre-incubated with DNA oligonucleotides complementary to either the 5′ or the 3′ terminal part of the substrate. As blocking of the 3′ end, in contrast to that of the 5′ end, impaired the degradation of the substrate RNA (data not shown), the results of these experiments are consistent with 3′–5′ exoribonuclease activity.

As the Dis3 protein in yeast contains endonucleolytic activity as well, mediated by the PIN domain, a similar activity assay was performed to investigate whether hDis3L1 also acts as an endoribonuclease. These experiments

were performed in the presence of $Mn^{2+}$, rather than $Mg^{2+}$, because this was earlier shown to be required for the endo-nucleolytic activity of PIN domain-containing proteins. The results showed that under these conditions, no endonucleolytic activity could be detected in these EGFP-hDis3L1 precipitates (Supplementary Figure S2).

To investigate whether the exoribonuclease activity associated with hDis3L1 is also associated with the exosome core, similar activity assays were performed, but now with material immunoaffinity purified with antibodies to exosome core component hRrp40. In addition, the lysates used for these experiments were prepared from cells treated with an hDis3L1-specific siRNA or with a control siRNA. If hDis3L1 is responsible for the exosome-associated exoribonuclease activity, knocking down the expression level of hDis3L1

was expected to reduce this activity. In agreement with the earlier observations, exosome complexes isolated with the anti-hRrp40 antibodies displayed exoribonuclease activity (Figure 4B). The siRNA-mediated depletion of hDis3L1 (the efficiency of which is shown in Supplementary Figure S3) led to a reduced exoribonuclease activity of anti-hRrp40 precipitates, strongly suggesting that hDis3L1 indeed contributes to the activity of the human exosome.

### RNB domain of hDis3L1 is mediating its exoribonuclease activity

The identification of an RNB domain in hDis3L1 (described above) suggested that this domain might be necessary for its exoribonuclease activity. To investigate this in more detail, one of the most highly conserved residues in this domain, the aspartate at position 486 was replaced by an asparagine (D486N). Substitution of the corresponding residue in other RNB domains has been shown to inhibit their exonuclease activity without interfering with RNA binding, as was initially found for RNase II (Amblar and Arraiano, 2005). This residue also corresponds to the D551 in the yeast Dis3 protein. Substitution of D551 of yeast Dis3 abolished its exoribonuclease activity, whereas the endonuclease activity remained unaffected (Dziembowski et al, 2007). Likewise, two additional hDis3L1 mutants were generated in which the two conserved aspartates in the putative PIN domain were substituted for asparagines (D62N and D166N). The expression of EGFP-fused hDis3L1 mutants in transfected HEp-2 cells was monitored by western blotting, revealing similar expression levels for all hDis3L1 mutant fusion proteins (Figure 4C). A ribonuclease assay with the immunoaffinity-purified hDis3L1 mutants (Figure 4D) showed that the D486N mutant was completely inactive, in contrast to the wild-type protein and

the PIN domain mutants, which showed similar levels of exonucleolytic degradation of the substrate RNA. These results indeed indicate that the RNB domain is involved in exonucleolytic RNA degradation by hDis3L1.

The abrogation of the exonucleolytic activity by the RNB domain mutation confirms that the activity observed in the in vitro ribonuclease assay is due to the presence of hDis3L1 and is not caused by a contaminating ribonuclease, which may non-specifically co-purify with hDis3L1.

### hDis3L1 is involved in rRNA degradation

The cytoplasmic localization of hDis3L1 suggested that it might be involved in the exoribonucleolytic degradation of RNAs in the cytoplasm. To investigate this possibility, the effect of hDis3L1 depletion on ribosomal RNA was studied. Degradation of rRNA in human cells involves the formation of truncated, transiently poly(A)-tailed molecules (Slomovic et al, 2006). An oligo(dT)-primed RT–PCR labelling procedure allows the detection of these truncated, poly(A)-tailed molecules derived from cytoplasmic 28S rRNA (Slomovic et al, 2010). hRrp40, PM/Scl-100 and hDis3L1 were knocked down and the effect of reduced levels of these proteins on the 28S rRNA degradation intermediates was determined by the RT–PCR procedure, which is schematically illustrated in Figure 5A. Controls for the cell fractionation are shown in Supplementary Figure S4, panel A. Western blotting or RT–PCR quantification, in case appropriate antibodies were lacking, showed a strong reduction of the silenced proteins (Supplementary Figure S4, panel B). The RT–PCR products were analysed by denaturing gel electrophoresis, which showed that knocking down hDis3L1 resulted in the accumulation of truncated 28S rRNA fragments, whereas no or only a very weak accumulation of these molecules was
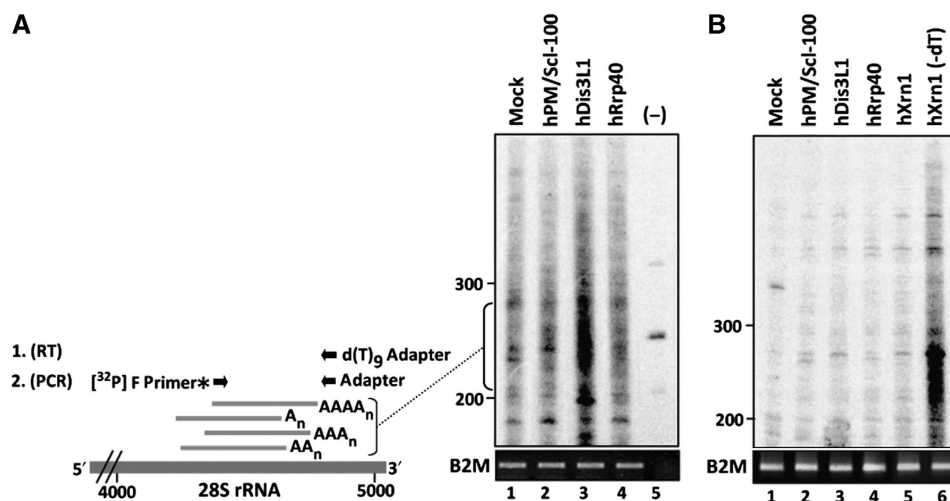


**Figure 5** Cytoplasmic accumulation of adenylated degradation intermediates after hDis3L1 knockdown. (**A**) Cytoplasmic RNA from cells in which the indicated proteins were silenced by RNAi was subjected to oligo(dT) RT–PCR labelling, followed by fractionation by denaturing polyacrylamide gel electrophoresis and autoradiography. A schematic representation of the labelling procedure is shown on the left. First, cDNA was generated using a d(T)$_9$-adapter primer. Products from these reactions were amplified by PCR using a [$^{32}$P]-labelled forward (F) primer corresponding to a sequence element of the 28S rRNA and a reverse primer corresponding to the adapter sequence. Material from a control reaction, in which the reverse transcriptase was omitted (−), is shown in lane 5. The positions of dsDNA markers are indicated on the left of the gel. For normalization, RT–PCR products obtained with PCR primers specific for the B2M gene are shown in the lower panel. (**B**) A similar oligo(dT) RT–PCR-labelling experiment as in panel **A**, but now the isolated RNA was incubated with oligo(dT) and RNase H before the RT reactions. RNA isolated from cells in which hXrn1 was knocked down, which similar to silencing of hDis3L1 leads to accumulation of poly(A) containing degradation intermediates, was used as a control to show that treatment with RNase H in the absence of oligo(dT) (lane 6) did not lead to the disappearance of the intermediates.

observed when hRrp40 or PM/Scl-100 were knocked down (Figure 5A). To verify whether the accumulated products were not artefacts of non-specific reverse transcription, the purified RNA purified was incubated with RNase H and oligo(dT) before the oligo(dT)-primed RT reaction. In this way, no cDNA can be produced as this treatment removes the poly(A) tails that are needed for the subsequent oligo(dT)-primed cDNA synthesis. The results of this experiment showed that this treatment indeed reduced the observed amplified signals to background levels (Figure 5B).

These results strongly suggest that hDis3L1 has a function in the degradation of rRNA and possibly other RNAs in the cytoplasm of human cells.

## Discussion

The evidence that the core of the eukaryotic exosome complex lacks exoribonuclease activity raised the question which proteins are responsible for this activity of the exosome. Paradoxically, the canonical human homologue of one of the main exosome-associated exoribonucleases in the yeast *Saccharomyces cerevisiae*, Dis3, does not detectably associate with the core of the exosome. In this study, a proteomic approach led to the identification of a novel hDis3L1, which is stably associated with human exosome complexes. The sequence of the Dis3L1 protein was first added to the databases in 2002, which may explain why it was not found in earlier proteomic analyses of purified exosome complexes (Chen *et al*, 2001). The failure to detect the association of hDis3 with the exosome complexes in the study of Chen and collaborators and also in other studies (Allmang *et al*, 1999a; Raijmakers *et al*, 2002) suggested that hDis3 is either weakly associated with the exosome core or not at all. The identification of hDis3L1 as an exosome-associated exoribonuclease indeed suggests that hDis3L1 shares more functional features with the yeast Dis3 protein than hDis3.

The ribonuclease assays presented in this study show that hDis3L1 is a $Mg^{2+}$-dependent exoribonuclease and that this activity is dependent on its RNB domain. On the other hand, no endoribonuclease activity was observed under conditions identical or similar to those earlier applied to study the endoribonuclease activity of the yeast Dis3 protein (Lebreton *et al*, 2008; Schaeffer *et al*, 2009). The failure to detect this activity is consistent with the relatively poor conservation of the PIN domain in hDis3L1, in which one of the three highly conserved aspartic acids is not present. These aspartic acids have been shown to be crucial for the endonucleolytic potential of PIN domains, as substitution of only one of these residues can severely reduce this activity (Glavan *et al*, 2006; Lebreton *et al*, 2008).

As hDis3L1 seems to accumulate in the cytoplasm, its subcellular localization only partially overlaps with that of the core exosome components, which are found in both the cytoplasm and the nucleus. Although the cytoplasmic accumulation of hDis3L1 was observed both with ectopically expressed GFP- and VSV-tagged proteins and with a polyclonal antibody to hDis3L1, our results to not exclude the possibility that a specific isoform of hDis3L1 displays another subcellular distribution. The sequence databases provide evidence for the existence of four isoforms, which most likely result from alternative splicing events. Future experiments

will have to clarify potential differences between their localization and function. The results of our localization studies not only suggest that hDis3L1 is specifically associated with cytoplasmic exosome complexes, but also implicate that the RNA substrates for hDis3L1 are restricted to the cytoplasm. Paradoxically, the yeast exosome-associated Dis3 protein is found both in the cytoplasm and in the nucleus (Synowsky *et al*, 2009). In view of the observations that the exosome core itself is catalytically inactive, it is tempting to speculate on the differentiation between ribonucleases associated with the nuclear and cytoplasmic core complexes. PM/Scl-100, which seems to be more concentrated in the nuclear compartment, might be more important for the nuclear functions of the exosome, whereas hDis3L1 might be more important for its cytoplasmic activities (such as the turnover of rRNAs and mRNAs). Interestingly, hDis3 seems to be mainly nucleoplasmic, suggesting that the function of the Dis3 protein in yeast is performed by separate homologous proteins, hDis3 and hDis3L1, in the nucleus and cytoplasm, respectively. In the nucleus, hDis3 seems to act independently of the core of the exosome, although an instable association that is not resistant to cell lysis and fractionation cannot be excluded (see also Supplementary Figure S5). The relationship with the third human member of the Dis3 protein family, hDis3L2, is currently enigmatic. The proteomic data suggest that also this protein is not stably associated with the core of the exosome, but more studies will be required to elucidate its function.

Besides differences in subcellular localization, the capacity of different exoribonucleases to degrade RNA substrates completely or to process RNA substrates to the mature 3′ end may differ from one enzyme to another. Indeed, it has been suggested earlier that one enzyme may take over from another to remove the last few nucleotides from an RNA substrate, and the dependence on the activity of the TRAMP complex seems to be different for the yeast Dis3 and Rrp6 proteins (LaCava *et al*, 2005).

The stable association of hDis3L1 with the human exosome suggests that it acts in concert with the core of the exosome in the degradation of cytoplasmic RNAs. Depletion of hDis3L1 led to a strong reduction of the exoribonuclease activity of immunoaffinity-purified exosome complexes, indicating that hDis3L1 is indeed mediating part of the RNA-degrading activity of the exosome. This does, however, not exclude the possibility that a subset of hDis3L1 is not exosome associated and degrades RNAs independently of the exosome. Interestingly, the binding of yeast Dis3 to the exosome core is mediated mainly by the PIN domain (Schneider *et al*, 2009), and in view of the structural similarity, it is likely that the interaction of hDis3L1 and the human exosome core is mediated by the same element. The exosome core may function to bind RNA substrates in its central channel and to lead these RNAs to the exoribonuclease site of hDis3L1 (Bonneau *et al*, 2009).

One of the RNA substrates that are degraded by the exosome-associated hDis3L1 seemed to be 28S rRNA. The degradation of this RNA proceeds through polyadenylated intermediates, which accumulated on hDis3L1 knockdown. Although these molecules were detected in the cytoplasmic fraction, our data do not rule out the possibility that they are generated in the nucleus and enter the cytoplasm in the hDis3L1 knockdown cells. The depletion of one of the exosome core components had a less pronounced effect on the

accumulation of these molecules, which may indicate that the association of hDis3L1 with the exosome core is either not necessary for this activity or that the knockdown of PM/Scl-100 and hRrp40 was not efficient enough to produce a similar level of accumulation. Further studies will be required to investigate the requirement of the exosome core in hDis3L1-mediated RNA degradation in more detail, to shed more light on the ratio between exosome associated and free hDis3L1, and to identify additional cellular RNA substrates for hDis3L1.

Recently, we were informed about an independent study by other investigators, who also identified hDis3L1 (termed as hDis3L in their study) as an exoribonuclease associated with the cytoplasmic exosome (Tomecki et al, 2010). The results of this study confirm our conclusions on the sub-cellular localization, exosome association and enzymatic activities of hDis3L1.

It is clear that more studies have to be performed to elucidate the possible differences between the nucleases associated with the nuclear and cytoplasmic exosome. The data presented in this study show that hDis3L1, rather than hDis3, is an exoribonuclease, which is stably associated with exosome core complexes and this protein is mainly localized in the cytoplasm of human cells.

# Materials and methods

### Purification of exosome complexes

Polyclonal anti-hRrp40 (H70) antibodies, affinity purified from rabbit serum H70 (Brouwer et al, 2001a) were coupled to protein A-agarose beads (Kem-En-Tec, Denmark) by incubation for 2 h at room temperature in PBS. After washing the beads three times with 0.2 M sodium borate, pH 9.0, the beads were incubated twice with 20 mM dimethyl pimelinidate dihydrochloride (DMP [Sigma]) in 0.2 M sodium borate, pH 9.0, by end-over-end rotation for 30 min. DMP was inactivated by washing the beads four times with 0.2 M ethanolamine, pH 8.0, after which the beads were washed three more times with PBS.

Five billion HeLa cells were resuspended in six volumes of lysis buffer (25 mM Tris–HCl, pH 7.5, 100 mM KCl, 1 mM dithiothreitol (DTT), 2 mM EDTA, 0.5 mM PMSF, 2 mM $Na_3VO_4$, 2 mM NaF, 10 mM $NaHPO_4$, 0.05% NP-40, containing a protease inhibitor cocktail [Complete, Roche]) and incubated for 30 min on ice. After sonication (three times 30 s at 0°C), cell lysates were centrifuged at 100 000 g for 1 h at 4°C and the supernatants were used immediately or stored at −70°C.

The anti-hRrp40 beads were washed twice with wash buffer (PBS, 0.35 M NaCl, 0.05% NP-40), followed by washing with elution buffer A (0.1 M glycine–HCl, pH 2.5, 0.05% NP-40, 0.5 M NaCl) and two additional wash steps with wash buffer. Subsequently, HeLa S100 extract ($1 \times 10^9$ cell equivalents) was added and incubated overnight at 4°C by end-over-end rotation. The beads were then washed twice with wash buffer, once with wash buffer containing 1 M NaCl, and again three times with wash buffer. Bound proteins were eluted by applying elution buffer A. Eluted fractions were neutralized immediately by adding 1 M Tris base and the proteins were concentrated by acetone precipitation. Precipitated proteins were dissolved in SDS sample buffer, separated by 12% SDS–PAGE and stained with colloidal Coomassie Brilliant Blue.

### LC-MS/MS

The gel containing the immunoaffinity-purified proteins was cut into 19 slices, proteins were reduced with 1,4-dithiothreitol (6.5 mM) and alkylated with iodoacetamide reagent (54 mM). After thorough washing, the gel slices were rehydrated in trypsin solution (10 ng/μl) on ice. After addition of 30 μl of $NH_4HCO_3$ (50 mM, pH 8.5), samples were digested for 16 h at 37°C. The supernatant of the digest was collected and the gel slices were washed for 15 min in 5% formic acid at room temperature, after which the supernatant was combined with the earlier fraction and stored at −20°C. All

LC-MS/MS analyses were performed on an LTQ-Orbitrap mass spectrometer (Thermo, San Jose, CA) connected to an Agilent 1200 series nano-LC system. Peptides were fractionated on C18 with a multi-step gradient of 0.6% HAc (solution A) and 0.6% HAc/80% acetonitrile (solution B). The mass spectrometer was operated in the data-dependent mode to automatically switch between MS and MS/MS. Raw MS data were converted to peak lists using Bioworks Browser software, version 3.1.1. The spectra were searched with Mascot against all human proteins in the Swissprot (v56.2) database with a precursor mass tolerance of 15 ppm and a product mass tolerance of 0.9 Da with trypsin as an enzyme, allowing two miscleavages. Peptide identifications were accepted with a Mascot score $>25$ and a P-value $<0.005$, corresponding to 1% false discovery rate as determined by decoy database searching.

### cDNA cloning and generation of the hDis3L1 expression constructs

The complete coding sequence of the largest isoform of hDis3L1 (GenBank accession number: NM_001143688) was isolated from a teratocarcinoma cDNA library by PCR using the following oligonucleotides: 5′-GGATCCCTCGAGATGCTGCAGAAGCGGGAGAA-3′ and 5′-GTCGACTCACCCGGGTATTCCATAATTGTTTGAAAC-3′. The resulting amplicon of 3229 basepairs was subsequently cloned into the pCR4-TOPO vector according to the manufacturer's guidelines (Invitrogen). The sequence of the selected clone was confirmed by DNA sequencing. N-terminal EGFP- and VSV-tagged hDis3L1 expression constructs and a C-terminal EGFP-tagged expression construct were made by subcloning the coding sequence into the pEGFP-C3 (Clontech), pCI-neo-5′-VSV (Promega) and pEGFP-N2 vectors (Clontech), respectively, using the restriction enzyme combinations: Xho I/Sal I, Xho I/Sal I and Xho I/Sma I, respectively.

### Transient transfection of HEp-2 cells and fluorescence microscopy

To express tagged hDis3L1 in a human cell line, $4 \times 10^6$ HEp-2 cells were transfected with 20 μg of plasmid DNA in 1 ml DMEM supplemented with 10% FCS by electroporation at 260 V and 950 μF using a Gene-Pulsar II (Bio-Rad). To increase expression levels, 5 mM sodium butyrate was added to the medium 24 h after transfection. Forty-eight hours after transfection, the cells were harvested by trypsinization, resuspended in lysis buffer (25 mM Tris–HCl, pH 7.5, 100 mM KCl, 1 mM EDTA, 0.5 mM PMSF, 0.05% NP-40, 1 mM DTT) and sonicated three times 30 s on ice. To study the subcellular localization of hDis3L1 and hDis3, HEp-2 cells were transfected in a similar manner, seeded on glass coverslips and fixed after 48 h with 3.7% paraformaldehyde. EGFP-fusion proteins were visualized directly, whereas the VSV-tagged proteins were detected indirectly by incubation with a monoclonal anti-VSV antibody after permeabilization of the cells, followed by Alexa Fluor 555-conjugated goat anti-mouse antibodies (Invitrogen). Incubations with antibodies were performed in PBS supplemented with 1% sheep serum. The localization of EGFP- and VSV-tagged proteins was monitored by fluorescence microscopy. For the localization of the endogenous proteins hDis3L1 and hRrp40, HEp-2 cells were seeded on glass coverslips and fixed with methanol. Antibody incubations (anti-hRrp40; anti-hDis3L1, H00115752-B01P (Abnova)) were performed as described above with the exception that Alexa Fluor 488-conjugated goat anti-rabbit or anti-mouse secondary antibodies (Invitrogen) were used for the detection of hRrp40. The nuclei of the cells were stained by incubation with the Hoechst 33342 (Invitrogen), diluted in PBS, for 3 min. Images were made on a confocal laser scanning microscope (TCS SP2 AOBS System, Leica-microsystems).

### siRNA treatment

siRNAs were purchased from Eurogentec. The sequences of the siRNAs for EGFP and hDis3L1 are 5′-CCAUGUAACCGUAAGAA UAdTdT-3′ and 5′-CGAGAAGCGCGAUCACAUGdTdT-3′, respectively. Transfection of HEp-2 cells with these siRNAs was performed essentially as described earlier (Schilders et al, 2005).

### Immunoprecipitation

Polyclonal rabbit anti-GFP antibodies or polyclonal rabbit anti-hRrp40 antibodies were coupled to protein A-agarose beads (Kem-En-Tec, Denmark) in IPP500 (500 mM NaCl, 10 mM Tris–HCl, pH 8.0, 0.05% NP-40) at room temperature for 1 h. Beads were washed

once with IPP500 and twice with IPP150 (150 mM NaCl, 10 mM Tris–HCl, pH 8.0, 0.05% NP-40). HEp-2 cell extract was incubated with the antibody-coupled beads for 2 h at 4°C. After washing the beads twice with IPP150 (or IPP1000 for the anti-hRrp40-coupled beads), bound proteins were either eluted with sample buffer for SDS–PAGE analysis, or were washed two more times with RNA degradation assay buffer (described below).

### Immunoblotting

For the detection of proteins on western blots, polyclonal rabbit antibodies (anti-GFP, anti-γ-tubulin, GTU-88 [Abcam]), polyclonal mouse antibodies (anti-hDis3L1) or monoclonal mouse antibodies (anti-hRrp4, 15B3 [ModiQuest], anti-GFP, JL-8 [BD Biosciences]) were diluted in blocking buffer (5% skimmed milk, PBS, 0.05% NP-40). Blots were incubated with these antibodies for 1 h at room temperature. Bound antibodies were detected by incubation with IRDye 800CW-conjugated polyclonal goat anti-mouse or goat anti-rabbit antibodies (Li-Cor) for 1 h in blocking buffer and visualization using an Odyssey Infrared Imaging System (Li-Cor).

### In vitro RNA degradation assays

RNA degradation assays were performed using a radiolabelled 267 nucleotide RNA substrate, which was obtained by in vitro transcription in the presence of $^{32}P$ α-UTP. This substrate RNA contained the human 5.8S rRNA sequence and the most 5′ 100 nucleotides of ITS2 (Schilders et al, 2005). After gel-purification of the RNA substrate, it was incubated for 2 h with the immunoprecipitated material at 37°C in RNA degradation buffer (20 mM HEPES, pH 7.5, 50 mM KCl, 1 mM DTT, 1 mM $Na_2HPO_4$) containing different concentrations of $Mg^{2+}$ or $Mn^{2+}$. Reactions were stopped by the addition of RNA-loading buffer (9 M urea, 0.1% bromophenol blue, 0.1% xylene cyanol), supplemented with 20% v/v phenol. Samples were analysed by denaturing polyacrylamide gel electrophoresis followed by autoradiography.

### In vivo 28S rRNA degradation analysis

HeLa cells were grown as a monolayer at 37°C, 5% CO$_2$ in DMEM (Sigma) supplemented with 10% foetal calf serum, 2 mM L-glutamine and penicillin–streptomycin (Slomovic and Schuster, 2008). Cells were transfected with 400 pmol siRNA duplex (PM/Scl-100: 5′-GUUUCGAGAGAAGAUUGAUdTdT-3′, hRrp40: 5′-CACGCAC AGUACUAGGUCAdTdT-3′) using lipofectamine 2000 (Invitrogen).

After 24 h, cells were detached with trypsin and replated, followed 24 h later by a second transfection with 800 pmol siRNA; 72 h after the initial transfection, cytoplasmic fractions were obtained from HeLa cells as earlier described (van Dijk et al, 2007). To assess accumulation of truncated adenylated 28S rRNA, oligo(dT)-primed cDNA was subjected to 25 PCR cycles using a 28S rRNA-specific forward primer coupled with the adapter oligo as follows: 1 min 95°C, 1 min 58°C and 1 min 72°C. Products of this PCR were used as templates in a second round of PCR-labelling using the same 28S rRNA primer, which was 5′ end [$^{32}P$] labelled by polynucleotide kinase and γ-[$^{32}P$]ATP and the adapter. This second round was performed as described above, but consisted of five cycles and was followed by 10 min of extension at 72°C. PCR-labelled products were resolved by 6% denaturing PAGE and autoradiography. Ethidium bromide-stained DNA markers were run on the same gels and used as length markers.

### Supplementary data

Supplementary data are available at The EMBO Journal Online (http://www.embojournal.org).

## Conflict of interest

The authors declare that they have no conflict of interest.

## References

Allmang C, Kufel J, Chanfreau G, Mitchell P, Petfalski E, Tollervey D (1999a) Functions of the exosome in rRNA, snoRNA and snRNA synthesis. EMBO J 18: 5399–5410

Allmang C, Petfalski E, Podtelejnikov A, Mann M, Tollervey D, Mitchell P (1999b) The yeast exosome and human PM-Scl are related complexes of 3′ → 5′ exonucleases. Genes Dev 13: 2148–2158

Amblar M, Arraiano CM (2005) A single mutation in Escherichia coli ribonuclease II inactivates the enzyme without affecting RNA binding. FEBS J 272: 363–374

Bonneau F, Basquin J, Ebert J, Lorentzen E, Conti E (2009) The yeast exosome functions as a macromolecular cage to channel RNA substrates for degradation. Cell 139: 547–559

Brouwer R, Allmang C, Raijmakers R, van AY, Vree Egberts W, Petfalski E, van Venrooij WJ, Tollervey D, Pruijn GJ (2001a) Three novel components of the human exosome. J Biol Chem 276: 6177–6184

Brouwer R, Pruijn GJ, van Venrooij WJ (2001b) The human exosome: an autoantigenic complex of exoribonucleases in myositis and scleroderma. Arthritis Res 3: 102–106

Callahan KP, Butler JS (2008) Evidence for core exosome independent function of the nuclear exoribonuclease Rrp6p. Nucleic Acids Res 36: 6645–6655

Chekanova JA, Shaw RJ, Wills MA, Belostotsky DA (2000) Poly(A) tail-dependent exonuclease AtRrp41p from Arabidopsis thaliana rescues 5.8 S rRNA processing and mRNA decay defects of the yeast ski6 mutant and is found in an exosome-sized complex in plant and yeast cells. J Biol Chem 275: 33158–33166

Chen CY, Gherzi R, Ong SE, Chan EL, Raijmakers R, Pruijn GJ, Stoecklin G, Moroni C, Mann M, Karin M (2001) AU binding proteins recruit the exosome to degrade ARE-containing mRNAs. Cell 107: 451–464

Clissold PM, Ponting CP (2000) PIN domains in nonsense-mediated mRNA decay and RNAi. Curr Biol 10: R888–R890

Dziembowski A, Lorentzen E, Conti E, Seraphin B (2007) A single subunit, Dis3, is essentially responsible for yeast exosome core activity. Nat Struct Mol Biol 14: 15–22

Edgar RC (2004) MUSCLE: multiple sequence alignment with high accuracy and high throughput. Nucleic Acids Res 32: 1792–1797

Frazao C, McVey CE, Amblar M, Barbas A, Vonrhein C, Arraiano CM, Carrondo MA (2006) Unravelling the dynamics of RNA degradation by ribonuclease II and its RNA-bound complex. Nature 443: 110–114

Glavan F, Behm-Ansmant I, Izaurralde E, Conti E (2006) Structures of the PIN domains of SMG6 and SMG5 reveal a nuclease within the mRNA surveillance complex. EMBO J 25: 5117–5125

Graham AC, Kiss DL, Andrulis ED (2009) Core exosome-independent roles for Rrp6 in cell cycle progression. Mol Biol Cell 20: 2242–2253

LaCava J, Houseley J, Saveanu C, Petfalski E, Thompson E, Jacquier A, Tollervey D (2005) RNA degradation by the exosome is promoted by a nuclear polyadenylation complex. Cell 121: 713–724

Lebreton A, Tomecki R, Dziembowski A, Seraphin B (2008) Endonucleolytic RNA cleavage by a eukaryotic exosome. Nature 456: 993–996

Lejeune F, Li X, Maquat LE (2003) Nonsense-mediated mRNA decay in mammalian cells involves decapping, deadenylating, and exonucleolytic activities. Mol Cell 12: 675–687

Letunic I, Doerks T, Bork P (2009) SMART 6: recent updates and new developments. *Nucleic Acids Res* **37:** D229–D232

Liu Q, Greimann JC, Lima CD (2006) Reconstitution, activities, and structure of the eukaryotic RNA exosome. *Cell* **127:** 1223–1237

Lorentzen E, Walter P, Fribourg S, Evguenieva-Hackenberg E, Klug G, Conti E (2005) The archaeal exosome core is a hexameric ring structure with three catalytic subunits. *Nat Struct Mol Biol* **12:** 575–581

Mitchell P, Petfalski E, Shevchenko A, Mann M, Tollervey D (1997) The exosome: a conserved eukaryotic RNA processing complex containing multiple 3′→5′ exoribonucleases. *Cell* **91:** 457–466

Noguchi E, Hayashi N, Azuma Y, Seki T, Nakamura M, Nakashima N, Yanagida M, He X, Mueller U, Sazer S, Nishimoto T (1996) Dis3, implicated in mitotic control, binds directly to Ran and enhances the GEF activity of RCC1. *EMBO J* **15:** 5595–5605

Raijmakers R, Vree Egberts W, van Venrooij WJ, Pruijn GJ (2002) Protein-protein interactions between human exosome components support the assembly of RNase PH-type subunits into a six-membered PNPase-like ring. *J Mol Biol* **323:** 653–663

Schaeffer D, Tsanova B, Barbas A, Reis FP, Dastidar EG, Sanchez-Rotunno M, Arraiano CM, van Hoof A (2009) The exosome contains domains with specific endoribonuclease, exoribonuclease and cytoplasmic mRNA decay activities. *Nat Struct Mol Biol* **16:** 56–62

Schilders G, Raijmakers R, Raats JM, Pruijn GJ (2005) MPP6 is an exosome-associated RNA-binding protein involved in 5.8S rRNA maturation. *Nucleic Acids Res* **33:** 6795–6804

Schilders G, van Dijk E, Raijmakers R, Pruijn GJ (2006) Cell and molecular biology of the exosome: how to make or break an RNA. *Int Rev Cytol* **251:** 159–208

Schneider C, Leung E, Brown J, Tollervey D (2009) The N-terminal PIN domain of the exosome subunit Rrp44 harbors endonuclease activity and tethers Rrp44 to the yeast core exosome. *Nucleic Acids Res* **37:** 1127–1140

Shiomi T, Fukushima K, Suzuki N, Nakashima N, Noguchi E, Nishimoto T (1998) Human dis3p, which binds to either GTP- or GDP-Ran, complements Saccharomyces cerevisiae dis3. *J Biochem* **123:** 883–890

Slomovic S, Fremder E, Staals RH, Pruijn GJ, Schuster G (2010) Addition of poly(A) and poly(A)-rich tails during RNA degradation in the cytoplasm of human cells. *Proc Natl Acad Sci USA* **107:** 7407–7412

Slomovic S, Laufer D, Geiger D, Schuster G (2006) Polyadenylation of ribosomal RNA in human cells. *Nucleic Acids Res* **34:** 2966–2975

Slomovic S, Schuster G (2008) Stable PNPase RNAi silencing: its effect on the processing and adenylation of human mitochondrial RNA. *RNA* **14:** 310–323

Synowsky SA, van WM, Raijmakers R, Heck AJ (2009) Comparative multiplexed mass spectrometric analyses of endogenously expressed yeast nuclear and cytoplasmic exosomes. *J Mol Biol* **385:** 1300–1313

Theobald DL, Mitton-Fry RM, Wuttke DS (2003) Nucleic acid recognition by OB-fold proteins. *Annu Rev Biophys Biomol Struct* **32:** 115–133

Tomecki R, Kristiansen MS, Lykke-Andersen S, Chlebowski A, Larsen KM, Szczesny RJ, Draskowska K, Pastula A, Andersen JS, Stepien PP, Dziembowski A, Jensen TH (2010) The human core exosome interacts with differentially localized processive RNases: hDIS3 and hDIS3L. *EMBO J* **29:** 2342–2357

van Dijk EL, Schilders G, Pruijn GJ (2007) Human cell growth requires a functional cytoplasmic exosome, which is involved in various mRNA decay pathways. *RNA* **13:** 1027–1035

van Hoof A., Frischmeyer PA, Dietz HC, Parker R, Allmang C (2002) Exosome-mediated recognition and degradation of mRNAs lacking a termination codon. *Science* **295:** 2262–2264

Waterhouse AM, Procter JB, Martin DM, Clamp M, Barton GJ (2009) Jalview Version 2—a multiple sequence alignment editor and analysis workbench. *Bioinformatics* **25:** 1189–1191